The Noise Level of Total Scattering Cross Section Measurement in a Reverberation Chamber

Qian Xu, Lei Xing, Yongjiu Zhao, Tian-Hong Loh, *Senior Member, IEEE*, Tianyuan Jia, and Yi Huang *Senior Member, IEEE*

***Abstract*—A reverberation chamber can be used to measure the total scattering cross section (TSCS) of an object, in which the time domain response needs to be analyzed to extract the scattering damping time. It has been observed in measurements that the noise level in extracting the scattering damping time is much higher than that in extracting the chamber decay time. The reasons behind this phenomenon are explored in this letter. Analytical distributions of the noise in TSCS measurements are derived and validated by measurements. Good agreements between analytical results and measurement results have been obtained, which gives guidelines on the prediction of noise level and the required independent sample number in the total scattering cross section measurement.**

***Index Terms*—total scattering cross section measurement, reverberation chamber, scattering damping time.**

I. Introduction

REVERBERATION chambers (RCs) are electrically large high-Q (reflective) cavities which have been widely used in electromagnetic compatibility (EMC) test [1], channel emulations [2-4], antenna measurements [5, 6] and material characterizations [7-13]. For the material characterizations, an RC can be used to measure the shielding effectiveness [7], dielectric properties [8], the absorption cross section (ACS) [9-11] and the total scattering cross section (TSCS) [12-16] of an object. These applications extend the use of RCs from EMC test to material measurements greatly.

An interesting phenomenon can be observed in the TSCS measurements: the noise level in TSCS measurement is much higher than that in the power delay profile (PDP) measurement. It seems that the noise levels are different for different measurement scenarios [15, 16], and no discussion has focused on it. Because the noise level could affect the measurement range of TSCS and has not been quantified yet, it is necessary to explore the insights behind the phenomenon and model the statistical behavior of it.

In this letter, Section II reviews the TSCS measurement procedure and focus on the noise level in the time domain response, Section III presents the analytical modeling of the statistical behavior of the noise, and compares the analytical results with the measurement results. Finally, discussion and conclusions are given in Section IV.

II. TSCS Measurement Setup

Figure 1 illustrates the equivalent TSCS measurement scenario of a stirrer. 'Equivalent' means the stirrer is not freely moved but is restricted (rotating around an axis), thus the measured TSCS is an equivalent TSCS [15]. The vector network analyzer (VNA) and the motor controller are controlled by the computer. Broadband antennas (Ant 1 and Ant 2) are connected to port 1 and port 2 of the VNA respectively. The stirrers are controlled to rotate in a step-wise mode, i.e. when the rotation of a stirrer is complete; S-parameters are recorded by the computer. A measurement workflow is given in Fig. 2(a). Suppose the equivalent TSCS of the horizontal (H-) stirrer is measured, we have to rotate (or move) the H-stirrer for a number of positions (N positions in Fig. 2(a)) and average the time domain response. To increase the measurement accuracy, this measurement process needs to be repeated for different antenna positions or vertical (V-) stirrer positions [12-14].

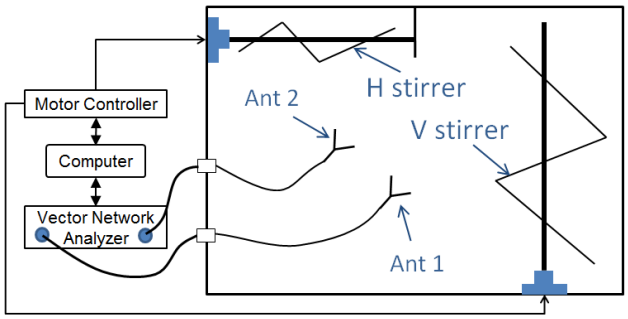

Fig. 1. A schematic plot of TSCS measurement setup in an RC.

Manuscript received *.

This work was supported in part by the National Natural Science Foundation of China (61701224 and 61601219) and Nature Science Foundation of Jiangsu Province (BK20160804).

Q. Xu, L. Xing, Y. Zhao are with College of Electronic and Information Engineering, Nanjing University of Aeronautics and Astronautics, Nanjing 211106, China (e-mail: emxu@foxmail.com).

T. –H. Loh is with Engineering, Materials & Electrical Science Department, National Physical Laboratory, Teddington, TW11 0LW, United Kingdom.

T. Jia and Y. Huang are with the Department of Electrical Engineering and Electronics, The University of Liverpool, Liverpool, L69 3GJ, UK.

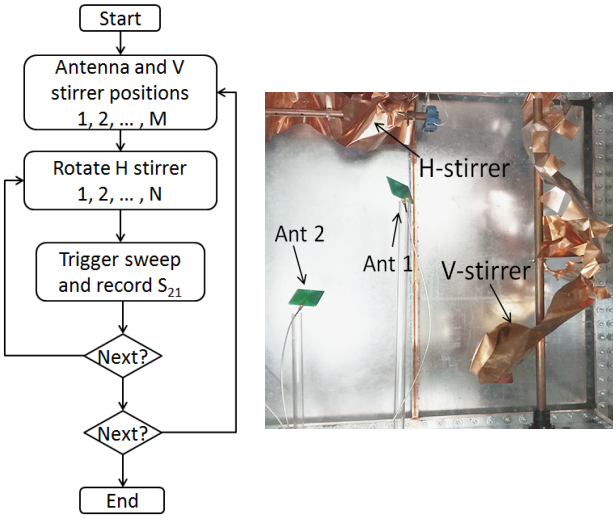

(a) (b)

Fig. 2. (a) TSCS measurement procedure for the H-stirrer, (b) measurement scenario setup in an RC. The RC dimensions are 1.2 m (length) × 0.8 m (width) × 1.2 m (height), the H-stirrer has a length of 66 cm and a diameter of 20 cm, the V-stirrer has a height of 115 cm and a diameter of 40 cm. The lowest usable frequency is about 1 GHz.

Mathematically, suppose $s(t)$ is the measured time domain response for one stirrer position between Ant 1 and Ant 2. $s(t)$ can be obtained from an oscilloscope directly [17] or from the inverse Fourier transform (IFT) of the measured S_{21} by using $s(t) = \text{IFT}(S_{21})$. The PDP can be measured using [9, 10]

$$\text{PDP}(t) = \langle [s(t)]^2 \rangle_L \tag{1}$$

where $\langle \cdot \rangle_L$ means the average for L scenarios with different stirrer or antenna positions. Because the PDP decays exponentially and the decay speed is determined by the chamber Q factor or chamber decay time τ_{RC}, (1) is normally used to extract the Q factor [5]. To measure the TSCS, we need to obtain $C(t)$ which is defined as the ratio of the unstirred power envelop to the PDP [12-14]

$$C(t) = \frac{\langle \langle s(t) \rangle_N^2 \rangle_M}{\text{PDP}(t)} = \frac{\langle \langle s(t) \rangle_N^2 \rangle_M}{\langle [s(t)]^2 \rangle_{N \times M}} \tag{2}$$

where N is the H-stirrer position number and M is the V-stirrer position number and antenna position number in Fig. 2(a), $\langle \cdot \rangle_N$ means the average for N H-stirrer positions when the V-stirrer is standstill, $\langle \cdot \rangle_M$ means the average for M V-stirrer and antenna positions, and $\langle \cdot \rangle_{N \times M}$ means the PDP is obtained using the average over $L = N \times M$ measurement scenarios. It has been given that $C(t)$ decays exponentially with a speed determined by the scattering damping time τ_s [12-16]

$$C(t) = e^{-t/\tau_s} \tag{3}$$

and the TSCS can be obtained from τ_s using [12-16]

$$\text{TSCS} = \frac{V}{\tau_s c_0} \tag{4}$$

where V is the volume of the RC and $c_0 = 3 \times 10^8\ m/s$ is the speed of light in free space.

To measure the equivalent TSCS of the H-stirrer, $N = 360$ and $M = 50$ (10 V-stirrer positions and 5 antenna positions) were used, S_{21} with 1601 frequency sample points were measured in the frequency range of 2.8 GHz – 3.0 GHz. The time domain response was obtained by applying the IFT to the measured S_{21}. The measured numerator and denominator (PDP) of (2) are shown in Fig. 3(a), and the measured $C(t)$ is illustrated in Fig. 3(b). It can be observed that the noise level of PDP is about 40 dB lower than the peak value, but the noise level of $C(t)$ in Fig. 3(b) is only about -15 dB lower than the peak value. Since we need to extract the chamber decay time τ_{RC} from the decay of the PDP, and extract the scattering damping time τ_s from the decay of $C(t)$ [12-16], a lower noise level means the extracted result has a higher accuracy. It is interesting to note that the noise level of $C(t)$ is much higher than that of the PDP, and this effect can also be found in the previous TSCS measurements [15, 16], but no discussion has been given yet.

To have a good understanding of this high noise level in $C(t)$ measurements, we apply an analytical approach to quantify it in the next section.

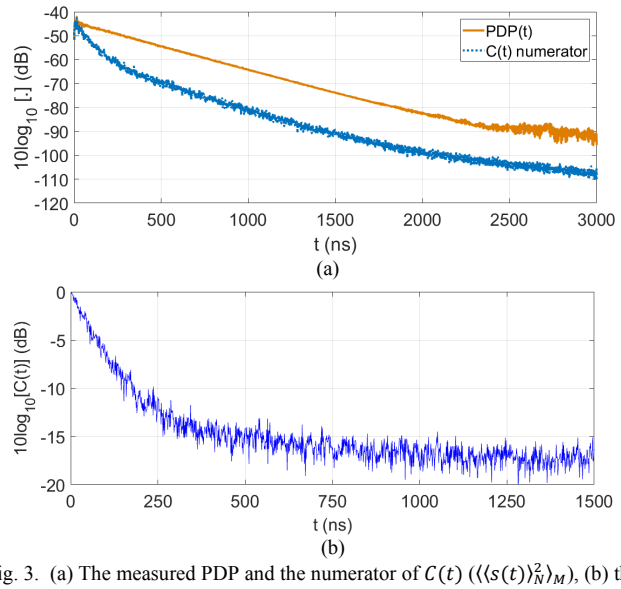

Fig. 3. (a) The measured PDP and the numerator of $C(t)$ ($\langle \langle s(t) \rangle_N^2 \rangle_M$), (b) the measured $C(t)$ for the H-stirrer.

III. Analytical Modeling

It has been found that the time domain response of the RC $s(t)$ can be modeled by using a nonstationary stochastic process [15], and the probability distribution function (PDF) can be expressed as [15]

$$\text{PDF}[s(t)] = \frac{1}{\sigma\sqrt{2\pi}} e^{-\frac{x^2}{2\sigma^2}} \tag{5}$$

which is a normal distribution where x is the variable for PDF$[x]$, σ is the standard deviation and varies with time. To

investigate the noise level of $C(t)$ in (2), we first analyze the numerator of $C(t)$.

From (5), suppose the independent sample number is N, we can obtain the PDF of $\langle s(t)\rangle_N$ as

$$\mathrm{PDF}[\langle s(t)\rangle_N] = \frac{\sqrt{N}}{\sigma\sqrt{2\pi}} e^{-\frac{Nx^2}{2\sigma^2}} \tag{6}$$

which is still a normal distribution, and the PDF of $\langle s(t)\rangle_N^2$ can be further obtained as

$$\mathrm{PDF}[\langle s(t)\rangle_N^2] = \frac{\sqrt{N}}{\sigma\sqrt{2\pi}} e^{-\frac{Nx}{2\sigma^2}} \tag{7}$$

We can find that the PDF of $\langle\langle s(t)\rangle_N^2\rangle_M$ is a gamma distribution

$$\mathrm{PDF}[\langle\langle s(t)\rangle_N^2\rangle_M] = \frac{x^{M/2-1}(MN)^{M/2}}{2^{M/2}\Gamma(M/2)\sigma^M} e^{-\frac{MNx}{2\sigma^2}} \tag{8}$$

where $\Gamma(\cdot)$ is the Gamma function $\Gamma(x) = \int_0^\infty v^{x-1}e^{-v}dv$. The mean value and the standard deviation of (8) can be derived as

$$\mathrm{Mean}[\langle\langle s(t)\rangle_N^2\rangle_M] = \frac{\sigma^2}{N} \tag{9}$$

$$\mathrm{Std}[\langle\langle s(t)\rangle_N^2\rangle_M] = \frac{\sigma^2\sqrt{2}}{N\sqrt{M}} \tag{10}$$

Similar to the derivation process from (5) to (10), we can obtain the PDF of the denominator (PDP) in (2) which is also a gamma distribution

$$\mathrm{PDF}[\mathrm{PDP}(t)] = \frac{x^{L/2-1}L^{L/2}}{2^{L/2}\Gamma(L/2)\sigma^L} e^{-\frac{Lx}{2\sigma^2}} \tag{11}$$

the mean value and the standard deviations are σ^2 and $\sigma^2\sqrt{2/L}$. For the PDP measurements, L is normally large and the standard deviation of the PDP can be very small. This can be observed in Fig. 3(a), nearly no statistical fluctuation is observed for the PDP as we used $N \times M = 18000$ sets of $s(t)$ to obtain the PDP. Finally, the PDF of $C(t)$ can be derived from (8) and (11) as

$$\mathrm{PDF}[C(t)] = \frac{\Gamma(L/2+M/2)L^{L/2}(MN)^{M/2}x^{M/2-1}}{\Gamma(L/2)\Gamma(M/2)(MNx+L)^{M/2+L/2}} \tag{12}$$

The mean value and the standard deviation are

$$\mathrm{Mean}[C(t)] = \frac{L}{N(L-2)} \tag{13}$$

$$\mathrm{Std}[C(t)] = \frac{L\sqrt{2}}{N(L-2)\sqrt{M}}\sqrt{\frac{M+L-2}{L-4}} \tag{14}$$

It can be found that when $L \to \infty$, (12) – (14) degenerates to (8) – (10) for $\sigma = 1$, respectively. Since the statistical behavior of $C(t)$ has been obtained, we can compare the theoretical predictions and the measurement results.

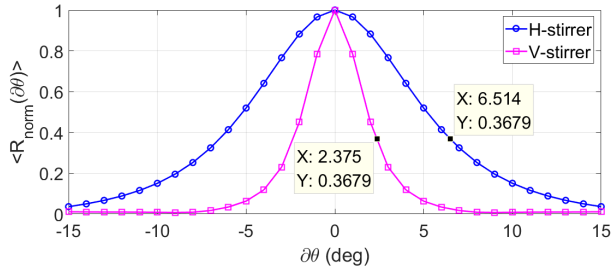

Fig. 4. Measured normalized average angular correlations for the H-stirrer and V-stirrer, a threshold of $1/e \approx 0.3679$ is used to obtain the correlated angle [1].

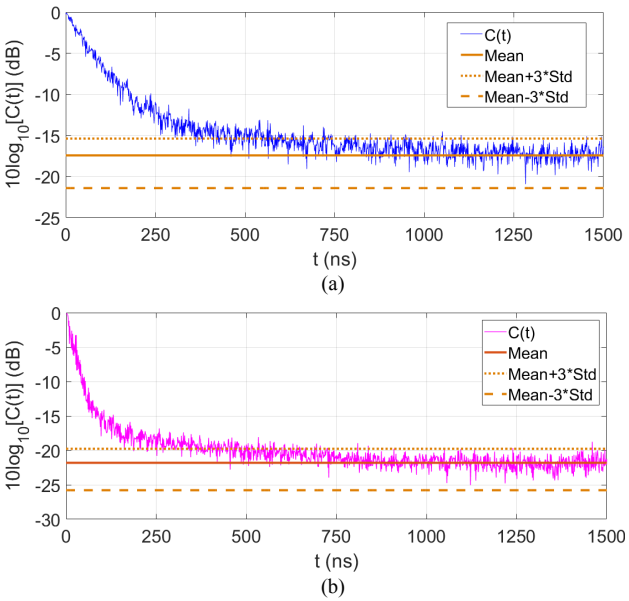

Fig. 5. (a) The measured $C(t)$ for the H-stirrer equivalent TSCS measurement; (b) the measured $C(t)$ for the V-stirrer equivalent TSCS measurement. The theoretical values are plotted in straight constant lines;

The first thing needs to do is to determine the independent sample number N. Note that the measured sample number does not mean the independent sample number. From the angular correlation R defined in [1]

$$R(\partial\theta) \equiv \int_{-360}^{360}[P_r(\theta) - \overline{P_r(\theta)}][P_r(\theta+\partial\theta) - \overline{P_r(\theta)}]d\theta \tag{15}$$

where $\partial\theta$ is the deviation of the rotation angle, $P_r = |S_{21}|^2$ is the receiving power for each rotation angle θ of the H-stirrer, and $\overline{P_r(\theta)}$ means the mean value of P_r over a 360° rotation. The angular correlation can be averaged over frequencies and antenna positions to give an averaged (smoothed) result. From the measured S-parameters, the normalized average angular correlation $\langle R_{norm}(\partial\theta)\rangle$ for the H-stirrer can be obtained and is plotted in Fig. 4. We have also repeated the TSCS measurement process for the V-stirrer, and $\langle R_{norm}(\partial\theta)\rangle$ for the V-stirrer is also presented. It can be seen from Fig. 4 that the correlated angle are 6.514° and 2.375° for the H-stirrer and the

V-stirrer respectively. Thus the independent sample numbers for the H-stirrer and V-stirrer are $N = 360°/6.514° \approx 55$ and $360°/2.375° \approx 152$ respectively.

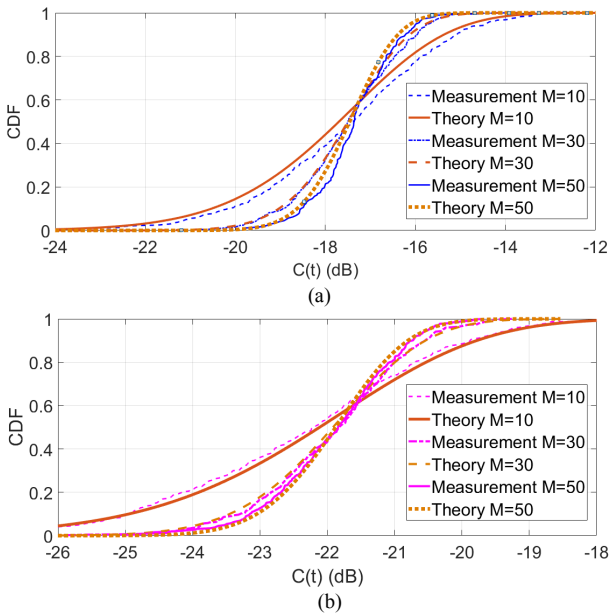

Fig. 6. (a) The measured and the theoretical CDFs of the noise in H-stirrer equivalent TSCS measurement *N*=55; (b) The measured and the theoretical CDFs of the noise in V-stirrer equivalent TSCS measurement *N*=152;

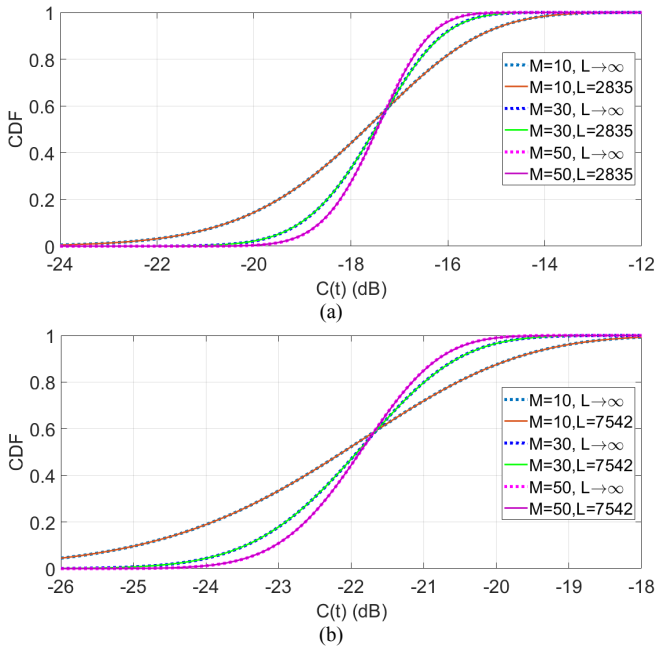

Fig. 7. (a) Theoretical CDFs of the noise in H-stirrer equivalent TSCS measurement *N*=55; (b) Theoretical CDFs of the noise in V-stirrer equivalent TSCS measurement *N*=152;

From (13) and (14), when $N = 55$, $M = 50$ and $L \to \infty$, the mean value and the standard deviation for the noise level in H-stirrer measurement can be calculated. The theoretical value and the measured noise level are compared in Fig. 5(a). Similarly, the noise level in V-stirrer measurement and the theoretical value are shown in Fig. 5(b). As can be seen, very good agreements have been obtained in both H- and V-stirrer measurement. The theoretical cumulative distribution function (CDF) of the noise can also be obtained using the numerical integral of the PDF in (12) for different M values. The measured CDF and the theoretical CDF for different M values are illustrated in Fig. 6. Not surprisingly, very good agreements have been obtained for both H- and V-stirrer measurement.

We have also checked the CDFs in Fig. 7 when a finite L is used. L for the H-stirrer and V-stirrer can be obtained from the standard deviation of the PDP in (11). Although 18000 sets of $s(t)$ are used, the independent sample number L are 2835 and 7542 for H- and V-stirrers respectively. As expected, for such large L, no significant difference is observed. These can also be confirmed by comparing the mean value and standard deviation in (9), (10) with (13), (14).

IV. Discussion and Conclusions

The noise level in the TSCS measurement affects the measurement accuracy of the TSCS. A low noise level means a longer time domain response can be used to extract the scattering damping time (τ_s), thus a more accurate TSCS can be obtained. Previous measurements show that this noise level could be different for different measurement scenarios and no investigation has been given. This study presents an analytical approach to this problem. Analytical derivations show that the mean value of the $C(t)$ noise is $1/N$, and the standard deviation is $\sqrt{2/M}/N$. The PDF and CDF of the noise have been obtained and compared with measurement results. Good agreements have been obtained.

This study can provide guidelines in TSCS measurement:

1) The required independent sample number can be predicted using the analytical equation. When the TSCS is large, $C(t)$ decays quickly and a lower noise level is required. Similarly, the standard deviation of the noise level can also be predicted.
2) A suitable RC volume is necessary. When the volume of the RC is too large, the independent sample number will reduce which will result in a high noise level. When the volume of the RC is too small, although the noise level is low, $C(t)$ could decay so quickly that not enough time domain response can be used to extract τ_s. A trade-off exists but can be quantified using the analytical equations.

References

[1] IEC 61000-4-21, Electromagnetic compatibility (EMC) – Part 4-21: Testing and measurement techniques – Reverberation chamber test methods, IEC Standard, Ed 2.0, 2011-01.

[2] E. Genender, C. L. Holloway, K. A. Remley, J. M. Ladbury and G. Koepke, "Simulating the multipath channel with a reverberation chamber: application to bit error rate measurements," *IEEE Transactions on Electromagnetic Compatibility,* vol. 52, no. 4, pp.766-777, Nov. 2010.

[3] C. L. Holloway, D. A. Hill, J. M. Ladbury, P. F. Wilson, G. Koepke and J. Coder, "On the Use of reverberation chambers to simulate a Rician radio environment for the testing of wireless devices," *IEEE Transactions on Antennas and Propagation*, vol. 54, no. 11, pp. 3167-3177, Nov. 2006.

[4] A. Sorrentino, A. Gifuni, G. Ferrara and M. Migliaccio, "Mode-stirred reverberating chamber autocorrelation function: model, multifrequency measurements and applications," *IET Science, Measurement & Technology*, vol. 9, no. 5, pp. 547-554, 2015.

[5] C. L. Holloway, H. A. Shah, R. J. Pirkl, W. F. Young, D. A. Hill and J. Ladbury, "Reverberation chamber techniques for determining the radiation and total efficiency of antennas," *IEEE Transactions on Antennas and Propagation*, vol. 60, no. 4, pp. 1758-1770, Apr. 2012.

[6] P. -S. Kildal, C. Carlsson and J. Yang, "Measurement of free-space impedances of small antennas in reverberation chambers," *Microwave and Optical Technology Letters*, vol. 32, pp. 112-115. 2002.

[7] C. L. Holloway, D. A. Hill, J. Ladbury, G. Koepke and R. Garzia, "Shielding effectiveness measurements of materials using nested reverberation chambers," *IEEE Transactions on Electromagnetic Compatibility*, vol. 45, no. 2, pp. 350-356, May 2003.

[8] P. Hallbjorner, U. Carlberg, K. Madsen, and J. Anderson, "Extracting electrical material parameters of electrically large dielectric objects from reverberation chamber measurements of absorption cross section," *IEEE Transactions on Electromagnetic Compatibility*, vol. 47, no. 2, pp. 291–303, May 2005.

[9] D. Senic, A. Sarolic, Z. M. Joskiewicz, and C. L. Holloway, "Absorption cross-section measurements of a human model in a reverberation chamber," *IEEE Transactions on Electromagnetic Compatibility*, vol. 58, no. 3, pp. 721–728, Jun. 2016.

[10] I. D. Flintoft, S. J. Bale, S. L. Parker, A. C. Marvin, J. F. Dawson, and M. P. Robinson, "On the measurable range of absorption cross section in a reverberation chamber," *IEEE Transactions on Electromagnetic Compatibility*, vol. 58, no. 1, pp. 22–29, Feb. 2016.

[11] A. Gifuni, G. Ferrara, A. Sorrentino and M. Migliaccio, "Analysis of the Measurement uncertainty of the absorption cross section in a reverberation chamber," *IEEE Transactions on Electromagnetic Compatibility*, vol. 57, no. 5, pp. 1262-1265, Oct. 2015.

[12] G. Lerosey and J. de Rosny, "Scattering cross section measurement in reverberation chamber," *IEEE Transactions on Electromagnetic Compatibility*, vol. 52, no. 2, pp. 280–284, May 2007.

[13] S. Lallechere, I. E. Baba, P. Bonnet, and F. Paladian, "Total scattering cross section improvements from electromagnetic reverberation chambers modelling and stochastic formalism," *5th European Conference on Antennas and Propagation (EUCAP)*, Rome, Italy, Apr. 2011, pp. 81–85.

[14] I. E. Baba, S. Lallechere, P. Bonnet, J. Benoit, and F. Paladian, "Computing total scattering cross section from 3-D reverberation chambers time modelling," *Asia-Pacific International EMC Symposium (APEMC)*, Singapore, May 2012.

[15] Q. Xu, Y. Huang, L. Xing, Z. Tian, M. Stanley and S. Yuan, "B-Scan in a reverberation chamber," *IEEE Transactions on Antennas and Propagation*, vol. 64, no. 5, pp. 1740-1750, May 2016.

[16] Q. Xu, Y. Huang, L. Xing, Z. Tian, C. Song and M. Stanley, "The limit of the total scattering cross section of electrically large stirrers in a reverberation chamber," *IEEE Transactions on Electromagnetic Compatibility*, vol. 58, no. 2, pp. 623-626, Apr. 2016.

[17] I. H. Naqvi and G. E. Zein, "Time domain measurements for a time reversal SIMO system in reverberation chamber and in an indoor environment," *IEEE International Conference on Ultra-Wideband*, Hannover, Germany, 2008, pp. 211-214.